Impact of modal dispersion on the performance of an SDM optical network

Nicola Sambo
TECIP
Scuola Superiore Sant'Anna,
Pisa, Itally
n.sambo@santannapisa.it

Chiara Lasagni
Università dell'Aquila
L'Aquila, Italy

Paolo Serena
Università di Parma
Parma, Italy

Piero Castoldi
TECIP
Scuola Superiore Sant'Anna,
Pisa, Itally

Alberto Bononi
Università di Parma
Parma, Italy

***Abstract*—Space-division multiplexing (SDM) is under investigation to support the growing capacity demand. Contrary to single-mode fibers, multi-core and multi-mode fibers supporting SDM experience a much higher modal dispersion (MD) that undermines the assumptions of quality of transmission (QoT) models usually unaware of it.**

In this paper, we investigate the impact of modal dispersion on SDM networks through an MD-aware Gaussian noise (GN) model. Network analysis shows that modal dispersion increases the throughput considering: i) Shannon limit, ii) different modulation formats.

***Index Terms*—SDM, multi-mode fibers, FMF, GN model, Shannon capacity.**

I. Introduction

Networks based on space-division multiplexing (SDM) with multi-core or multi-mode fibers are under investigation to support the growing capacity demand. Several limitations have already been resolved, such as linear inter-modal crosstalk and modal dispersion (MD), which are efficiently equalized by multiple-input multiple-output (MIMO) coherent receivers [1], [2]. Commercial add&drop multiplexers are already available on the market handling 15 modes with multiplane light conversion technology [3], [4]. Network performance has been evaluated in few-mode fiber (FMF)-based SDM networks with partial mode switching, thus avoiding full-MIMO while offering more network flexibility [5]. Quality of transmission studies have been performed extending the widely adopted Gaussian Noise (GN) model [6], [7] to account for inter-modal crosstalk [8]. The GN model is conservative, assuring that established channels do not experience worse physical layer performance than the estimated ones, thus avoiding possible outages. However, the basic GN model does not account for the interplay between MD and the Kerr nonlinearity. Such an interplay has been shown in the limit of high MD [9] to be beneficial in mitigating the nonlinear effect, provided that linear MD is fully compensated at the receiver. An extension of the GN model to include arbitrary values of MD in strongly coupled SDM fibers has been recently shown and validated in [10], with both a semi-analytical and a simplified formula.

In this paper, we use the extended GN model (accounting for MD) to investigate for the first time the gain brought by MD in improving the performance of an SDM network. We will show the benefit of MD/Kerr interaction in network environments from different perspectives. First, the Shannon limit will be analyzed at varying the number of modes and the amount of modal dispersion. Then, the network capacity will be analyzed in a network supporting multiple modulation formats: N-ary polarization multiplexing quadrature amplitude modulation (PM-NQAM), with $N = 8, 16, 32, 64$, and PM-quadrature phase-shift keying (PM-QPSK).

This work has been supported by the MIUR PRIN2017 "FIRST" Project (GA 2017HP5KH7_002).

II. Physical layer modelling

The spatial modes in fibers supporting SDM experience both linear and nonlinear crosstalk. While the first can be equalized by the MIMO, the second leaves a nonlinear interference (NLI) usually dominated by cross-channel nonlinearity. If MIMO is available, a way to mitigate the nonlinearity is by minimizing the coherent accumulation of nonlinear effects along propagation. This can be done by maximizing the mode crosstalk, e.g., through strongly coupled multi-core or multi-mode fibers [9]. In this framework, even MD alleviates the nonlinear accumulation by decorrelating interfering channels. While in single-mode fibers the small MD does not play a significant role, the MD strength is hundred of times higher in SDM [11], thus changing the game. Although the interaction between MD and Kerr effect is random, in [10] it was shown that at the typical values of MD for strongly coupled SDM networks only the average NLI variance matters, and a formula to estimate it was proposed. The generalized signal-to-noise ratio (GSNR) – here adopted as figure of merit for quality of transmission – after MIMO is thus:

$$\text{GSNR} = \frac{P}{\sigma^2_{\text{ASE}} + \mathbb{E}\left[\sigma^2_{\text{NLI}}\right]}$$

with P signal power, σ^2_{ASE} the variance of amplified spontaneous emission noise, σ^2_{NLI} the NLI variance, and $\mathbb{E}$ indicating expectation with respect to MD. Thanks to the expectation, the MD has been included in the GN model without compromising the computational time [10]. The GSNR can be converted into achievable information rate C. Here we evaluate C by using the Shannon formula, which is an achievable limit by a detector matched to an additive white Gaussian noise channel. For each polarization tributary, we thus have

978-3-903176-44-7

TABLE I
ASSUMED MODULATION FORMATS: LINE RATE PER MODE AND GSNR THRESHOLD (TH)

Modulation format	Supported rate per mode	TH
PM-64QAM	768 Gb/s	24.6 dB
PM-32QAM	640 Gb/s	21.6 dB
PM-16QAM	512 Gb/s	18.6 dB
PM-8QAM	384 Gb/s	16 dB
PM-QPSK	256 Gb/s	12 dB

$C = \log_2(1 + \text{GSNR})$ [bits/symbol]. Thanks to such a model, we can estimate the gain brought by MD in mitigating the NLI in an SDM network.

III. Network performance

The network performance is evaluated on two network topologies: the mesh Spanish backbone in [12] and a ring of 20 nodes. The following assumptions are adopted: spans of 80 km, 64-Gbaud symbol rate, 75-GHz channels spacing, 6.5 dB of amplifier noise figure per mode, a span loss of 17.6 dB, chromatic dispersion 17 ps/nm/km, fiber nonlinear index $n_2 = 2.5 \cdot 10^{-20}$ m^2/W, Manakov correction factor as in [9, eq. (65)], transmission over the whole C band. The impact of MD is evaluated at a spatial mode dispersion (SMD) of 3 and 8 $\text{ps}/\sqrt{\text{km}}$ [11]. Channel power is optimized according to [13]. First, an analysis of the Shannon capacity limit is carried out, then, the achievable capacity constrained to the support of a specific set of modulation formats is evaluated.

A. Shannon capacity limit

The Shannon capacity limit C (per mode per polarization) is computed with a GSNR including non-linear effects in the presence of modal dispersion (3 or 8 $\text{ps}/\sqrt{\text{km}}$) or without it. Figure 1 shows the Shannon limit in bits/symbol averaged on all the possible network paths over the mesh (Fig. 1a) and the ring (Fig. 1b) topologies vs. the number of SDM modes. We note that the inclusion of MD implies a higher GSNR, thus a higher Shannon capacity. The Shannon limit increases with modal dispersion and with the number of modes offered by the fiber spans. In general, the mesh network can achieve a higher capacity since the ring presents a more limited connectivity implying longer routes. As an example, in the mesh topology with 16 modes, C is 8.4 bit/symbol (per polarization and per mode) without considering modal dispersion, while it is 8.6 bit/symbol (per polarization and per mode) with a modal dispersion of 8 $\text{ps}/\sqrt{\text{km}}$. Consequently, in the case of channels approaching the Shannon capacity, for instance with adaptive code-rate and probabilistic shaping, MD improves the capacity of a single spatial super-channel by about 400 Gb/s with 16 modes, two polarizations, and 64 Gbaud symbol rate.

B. Achievable network capacity constrained to supported modulation formats

Evaluations are carried out considering a set of possible modulation formats, each one supporting a specific gross rate per mode (assuming 64-Gbaud symbol rate) and each one associated to a minimum GNSR threshold (TH) value. Thresholds are taken from [14]. Tab. I summarizes the considered modulation formats with the associated gross rate per mode and the assumed TH on GSNR. Connection requests follow a Poisson distribution with mean inter-arrival time $1/\lambda$ and a holding time exponentially distributed with average $1/\mu = 250$s. Network load (λ/μ) is varied through λ. Path computation is performed with load balancing as in [15] and spectrum assignment is first fit. Each connection is switched over a bandwidth of 75 GHz. Depending on the selected path, the most spectral efficient modulation format supported by the computed GSNR over that path (with or without modal dispersion) is chosen. Then, based on the modulation format, a connection carries a specific rate, as previously mentioned. Results are shown considering loads guaranteeing a connection blocking probability lower than 10^{-2}. Table II shows the overall rate supported by the network without or in the presence of modal dispersion (8 $\text{ps}/\sqrt{\text{km}}$), assuming 16 modes in the two network topologies.

The overall rate increases with the network load, since more connections are active in the network. Modal dispersion permits to increase the overall capacity. Indeed, the higher GSNR values permit to use higher-order modulation formats. The improvement can be achieved by modifying the GN model as in [10], at comparable computational effort. As an example, in the ring topology, with 250 Erlang, an increase of 39 Tb/s more is supported by the network.

IV. Conclusions

We evaluated the impact of modal dispersion on the capacity of upcoming SDM networks exploiting strongly coupled spatial modes. To this purpose, we exploited a GN model extended to account for the interplay between the modal dispersion and the Kerr effect. The Shannon limit has been analyzed, showing a capacity increase (that could bring on average to a spatial super-channel capacity increase of 400 Gb/s). Then, the network capacity has been investigated considering multiple modulation formats showing an overall network capacity increase of up to 39 Tb/s in the assumed network scenarios.

V. Acknowledgement

This work has been supported by the MIUR PRIN2017 “FIRST” Project (GA 2017HP5KH7_002).

References

[1] S. Randel, R. Ryf, A. Sierra, P. J. Winzer, A. H. Gnauck, C. A. Bolle, R.-J. Essiambre, D. W. Peckham, A. McCurdy, and R. Lingle, “6×56-Gb/s mode-division multiplexed transmission over 33-km few-mode fiber enabled by 6×6 MIMO equalization,” *Opt. Express*, vol. 19, no. 17, pp. 16 697–16 707, Aug 2011.

[2] R. Ryf, S. Randel, A. H. Gnauck, C. Bolle, A. Sierra, S. Mumtaz, M. Esmaeelpour, E. C. Burrows, R.-J. Essiambre, P. J. Winzer, D. W. Peckham, A. H. McCurdy, and R. Lingle, “Mode-division multiplexing over 96 km of few-mode fiber using coherent 6×6 MIMO processing,” *Journal of Lightwave Technology*, vol. 30, no. 4, pp. 521–531, 2012.

[3] G. Labroille, P. Jian, N. Barre, B. Denolle, and J.-F. Morizur, “Mode selective 10-mode multiplexer based on multi-plane light conversion,” in *2016 Optical Fiber Communications Conference and Exhibition (OFC)*, no. Th3E.5, 2016.

[4] “Cailabs – Proteus-C,” https://www.cailabs.com/en/product/proteus-c/.

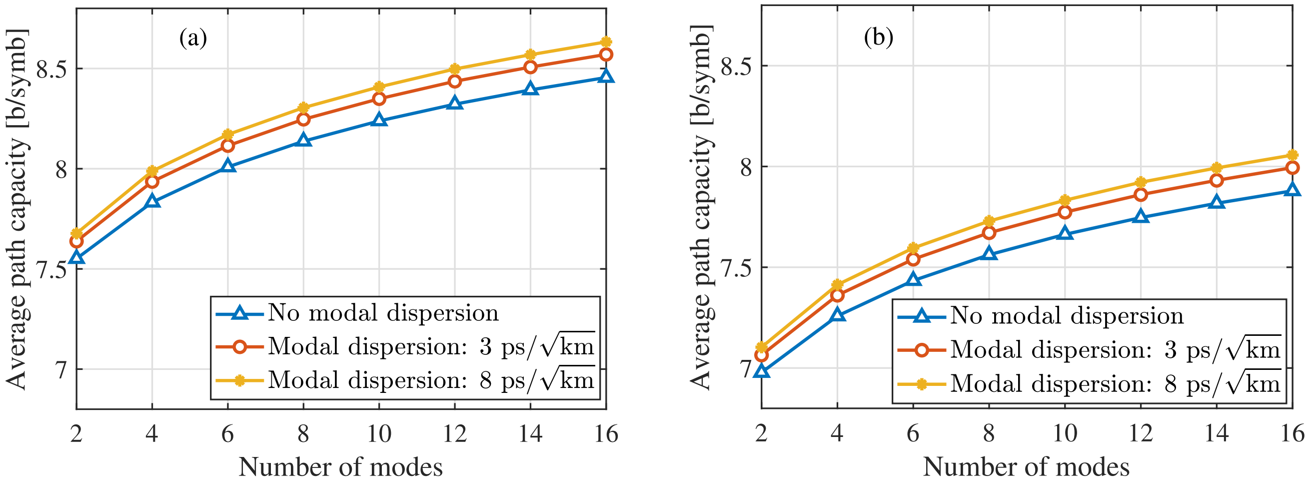

Fig. 1. Average path Shannon Capacity in: (a) the mesh topology; (b) the ring topology.

TABLE II
AVERAGE OVERALL NETWORK RATE [TB/S] IN: (A) THE MESH TOPOLOGY; (B) THE RING TOPOLOGY.

(a) Overall rate in the meshed topology

	No Modal Dispersion	**8ps/sqrt(km)**
100 Erlang	852.1 Tb/s	855.0 Tb/s
150 Erlang	1283.3 Tb/s	1287.6 Tb/s
200 Erlang	1704.3 Tb/s	1710.8 Tb/s
250 Erlang	2130.4 Tb/s	2137.5 Tb/s

(b) Overall rate in the ring topology

	No Modal Dispersion	**8ps/sqrt(km)**
100 Erlang	759.5 Tb/s	775.6 Tb/s
150 Erlang	1143.8 Tb/s	1168.1 Tb/s
200 Erlang	1517.6 Tb/s	1549.8 Tb/s
250 Erlang	1870 Tb/s	1909.5 Tb/s

[5] N. Sambo, P. Martelli, P. Parolari, A. Gatto, P. Castoldi, and P. Boffi, "Mode-group division multiplexing for provisioning in SDM networks," in *2020 European Conference on Optical Communication (ECOC)*, no. We2H6, 2020.

[6] A. Carena, V. Curri, G. Bosco, P. Poggiolini, and F. Forghieri, "Modeling of the impact of nonlinear propagation effects in uncompensated optical coherent transmission links," *Journal of Lightwave Technology*, vol. 30, no. 10, pp. 1524–1539, 2012.

[7] P. Poggiolini, G. Bosco, A. Carena, V. Curri, Y. Jiang, and F. Forghieri, "The GN-model of fiber non-linear propagation and its applications," *Journal of Lightwave Technology*, vol. 32, no. 4, pp. 694–721, 2014.

[8] P. Martelli and P. Boffi, "Crosstalk-induced penalty in coherent space-division multiplexing transmission," in *2018 20th International Conference on Transparent Optical Networks (ICTON)*, no. We.C1.4, 2018.

[9] C. Antonelli, M. Shtaif, and A. Mecozzi, "Modeling of nonlinear propagation in space-division multiplexed fiber-optic transmission," *Journal of Lightwave Technology*, vol. 34, no. 1, pp. 36–54, 2016.

[10] P. Serena, C. Lasagni, A. Bononi, C. Antonelli, and A. Mecozzi, "A model of the nonlinear interference in space-division multiplexed systems with arbitrary modal dispersion," in *2021 European Conference on Optical Communication (ECOC)*, no. Tu2D3, 2021.

[11] T. Hayashi *et al.*, "Field-deployed multi-core fiber testbed," in *Proc. of OECC and PSC*, no. PDP3, 2019.

[12] N. Sambo, A. Ferrari, A. Napoli, N. Costa, J. Pedro, B. Sommerkorn-Krombholz, P. Castoldi, and V. Curri, "Provisioning in multi-band optical networks," *Journal of Lightwave Technology*, vol. 38, no. 9, pp. 2598–2605, 2020.

[13] P. Poggiolini, G. Bosco, A. Carena, V. Curri, Y. Jiang, and F. Forghieri, "The GN-model of fiber non-linear propagation and its applications," *J. Light. Technol.*, vol. 32, no. 4, pp. 694–721, 2013.

[14] A. Mitra, D. Semrau, N. Gahlawat, A. Srivastava, P. Bayvel, and A. Lord, "Effect of channel launch power on fill margin in C+L band elastic optical networks," *Journal of Lightwave Technology*, vol. 38, no. 5, pp. 1032–1040, 2020.

[15] N. Sambo, F. Cugini, G. Bottari, G. Bruno, P. Iovanna, and P. Castoldi, "Lightpath provisioning in wavelength switched optical networks with flexible grid," in *2011 European Conference on Optical Communication (ECOC)*, no. We.10.P1.96, 2011.